AIP | Journal of Applied Physics

Description of Crystallite Orientation in Polycrystalline Materials. III. General Solution to Pole Figure Inversion

RyongJoon Roe

Citation: Journal of Applied Physics **36**, 2024 (1965); doi: 10.1063/1.1714396
View online: http://dx.doi.org/10.1063/1.1714396
View Table of Contents: http://scitation.aip.org/content/aip/journal/jap/36/6?ver=pdfcov
Published by the AIP Publishing

Description of Crystallite Orientation in Polycrystalline Materials. III. General Solution to Pole Figure Inversion

RYONG-JOON ROE
Electrochemicals Department, E. I. du Pont de Nemours Company, Inc., Niagara Falls, New York
(Received 23 October 1964)

A method is presented here by which orientation distribution of crystallites in anisotropic polycrystalline samples can be derived from a set of plane-normal distributions obtained by x-ray diffraction measurements. It is the generalization of the similar procedure proposed previously for analysis of samples having fiber texture. It thus represents a completely general solution to the problem of pole figure inversion, applicable to samples having any arbitrary symmetry elements. The plane-normal distribution function is expanded in a series of spherical harmonics, the coefficients of which, Q_{lm}^{i}, can be determined by numerical integration of experimental diffraction data. The crystallite distribution function is expanded in a series of generalized spherical harmonics which appear as solutions to the Schrödinger wave equation of a symmetric top. The coefficients of the crystallite distribution function, W_{lmn}, are then obtained as linear combinations of Q_{lm}^{i}. Symmetry properties of W_{lmn} arising from crystallographic or statistical symmetry elements existing in the sample are examined. The methods of estimating the series truncation errors and of minimizing the experimental error by a least-squares method, previously proposed in connection with fiber texture analysis, are still applicable here with appropriate generalizations. In addition it is shown that the effect of diffraction line broadening due to finite size or imperfection of crystallites can also be allowed for at least approximately.

I. INTRODUCTION

IN anisotropic polycrystalline materials, such as fibers, polymeric films, and rolled metals, knowledge of the distribution of crystallite orientations is often of theoretical and practical importance. When measurements are made on the variation of diffracted x-ray intensities, at a fixed Bragg angle, as a function of the relative orientation of the sample with respect to the diffractometer geometry, one obtains information concerning the orientation distribution of the particular crystallographic plane concerned throughout the sample. Such data are often presented as a stereographic projection of the plane-normals, which is called a pole figure diagram.[1] A collection of such diagrams, each pertaining to a different plane-normal, does not, however, reveal the crystallite orientation distribution directly by itself, since the correlations between the diagrams, demanded by the lattice structure of the crystallites, are not brought out explicitly. The present work is concerned with the method of deriving the quantitative representation of the crystallite orientation distribution by reduction of a set of x-ray diffraction data such as pole figure diagrams. The resulting distribution function can be interpreted as the analytical or numerical representation of the inverse pole figure.[2,3] The latter is obtained if we imagine that all the crystallites are rearranged so as to have their crystallographic axes coinciding and then the corresponding distribution of the reference axes of the sample is plotted. Earlier attempts at devising procedures for constructing the inverse pole figure either involved a trial and error method[4] or were confined to cubic crystals.[5] In a previous paper[6] (Part I of the present series) we have proposed a general method of pole figure inversion applicable to samples having fiber texture. In a subsequent paper[7] (Part II) the method was successfully applied to analyzing the crystallite orientation distribution in uniaxially strained samples of crosslinked polyethylene. The method is now extended so as to apply to all anisotropic materials without the restriction of cylindrical symmetry. It thus represents a completely general solution to the problem of pole figure inversion.

Efforts have been made here to preserve the notations used in the previous papers,[6,7] but some minor changes were unavoidable. The most important among them is the revised definition of $P_l^m(z)$ for negative values of m (see Appendix). In any case all the symbols are redefined here in order to make this paper self-contained.

II. CRYSTALLITE ORIENTATION DISTRIBUTION FUNCTION

The orientation of a crystallite in the polycrystalline sample is specified by means of Eulerian angles θ, ψ, and ϕ. In Fig. 1, 0-xyz is the system of orthogonal reference axes arbitrarily fixed in the polycrystalline sample and 0-XYZ is the same fixed in the crystallite. The angles θ and ψ define the orientation of the crystallite Z axis in the sample space, and ϕ specifies the rotation of the crystallite around its own Z axis. A more detailed definition of these angles is given in Part I. θ, ψ, and ϕ defined here are equivalent to β, α, and γ, respectively, given in the book by Margenau and Murphy.[8] The

[1] H. P. Klug and L. E. Alexander, *X-Ray Diffraction Procedures* (John Wiley & Sons, Inc., New York, 1954), Chap. 10.
[2] G. B. Harris, Phil. Mag. **43**, 113 (1952).
[3] M. H. Mueller, W. P. Chernock, and P. A. Beck, Trans. AIME **212**, 39 (1958).
[4] L. K. Jetter, C. J. McHargue, and R. O. Williams, J. Appl. Phys. **27**, 368 (1956).
[5] H. J. Bunge, Monatsber. Deut. Akad. Wiss. Berlin **1**, 27, 400 (1959); **3**, 97 (1961).
[6] R.-J. Roe and W. R. Krigbaum, J. Chem. Phys. **40**, 2608 (1964).
[7] W. R. Krigbaum and R.-J. Roe, J. Chem. Phys. **41**, 737 (1964).
[8] H. Margenau and G. M. Murphy, *The Mathematics of Physics and Chemistry* (D. Van Nostrand Company, Inc., New York, 1943), p. 272.

orientation distribution function of all crystallites in the sample is then represented by $w(\xi,\psi,\phi)$, where

$$\xi=\cos\theta \tag{1}$$

and

$$\int_0^{2\pi}\int_0^{2\pi}\int_{-1}^{1} w(\xi,\psi,\phi)d\xi d\psi d\phi=1. \tag{2}$$

Next we consider the ith reciprocal lattice vector $\mathbf{r}_i$ belonging to a crystallite. The orientation of $\mathbf{r}_i$ with respect to the crystallite coordinate system 0-XYZ is given by the polar angle Θ_i and the azimuthal angle Φ_i (see Fig. 2). Similarly, the orientation of $\mathbf{r}_i$ with respect to the sample coordinate system 0-xyz is specified by the polar angle χ_i and the azimuthal angle η_i (see Fig. 3). The two sets of angles (Θ_i,Φ_i) and (χ_i,η_i) referring to the same vector $\mathbf{r}_i$ can be related to each other through Eq. (3) which describes the transformation of cartesian coordinates accompanying the rotation of coordinate axes by ψ, θ, and ϕ.

$$\begin{bmatrix}\sin\chi_i\cos\eta_i\\ \sin\chi_i\sin\eta_i\\ \cos\chi_i\end{bmatrix}=\mathbf{T}^{-1}(\psi,\theta,\phi)\begin{bmatrix}\sin\Theta_i\cos\Phi_i\\ \sin\Theta_i\sin\Phi_i\\ \cos\Theta_i\end{bmatrix}, \tag{3}$$

where

$$\mathbf{T}(\psi,\theta,\phi)=\begin{bmatrix}\cos\psi\cos\theta\cos\phi-\sin\psi\sin\phi & \sin\psi\cos\theta\cos\phi+\cos\psi\sin\phi & -\sin\theta\cos\phi\\ -\cos\psi\cos\theta\sin\phi-\sin\psi\cos\phi & -\sin\psi\cos\theta\sin\phi+\cos\psi\cos\phi & \sin\theta\sin\phi\\ \cos\psi\sin\theta & \sin\psi\sin\theta & \cos\theta\end{bmatrix}. \tag{4}$$

The angles Θ_i and Φ_i can be calculated for each Miller index (hkl) from the unit cell dimensions and the crystal class of the crystallites. The angles χ_i and η_i specify the relative orientation of the sample with respect to the incident and diffracted x-ray beams. Let $I(\zeta_i,\eta_i)$ be the intensity of diffracted x-ray measured (at a fixed Bragg angle) as a function of the orientation of the sample and then corrected for various aberrations. Here

$$\zeta_i=\cos\chi_i. \tag{5}$$

The plane-normal orientation distribution $q_i(\zeta_i,\eta_i)$ is then obtained by normalization of the intensity function $I(\zeta_i,\eta_i)$; thus

$$q_i(\zeta_i,\eta_i)=I(\zeta_i,\eta_i)\Big/\int_0^{2\pi}\int_{-1}^{1} I(\zeta_i,\eta_i)d\zeta_i d\eta_i. \tag{6}$$

Various intensity corrections required for the purpose have recently been examined in detail by Bragg and Packer.[9]

Our purpose is to develop a procedure by which we can deduce the crystallite orientation distribution $w(\xi,\psi,\phi)$ from the set of plane-normal orientation distributions $q_i(\zeta_i,\eta_i)$ obtained experimentally. For this end we expand $q_i(\zeta_i,\eta_i)$ and $w(\xi,\psi,\phi)$ in a series of spherical harmonics and generalized spherical harmonics, respectively:

$$q_i(\zeta_i,\eta_i)=\sum_{l=0}^{\infty}\sum_{m=-l}^{l} Q_{lm}{}^iP_l{}^m(\zeta_i)e^{-im\eta_i} \tag{7}$$

and

$$w(\xi,\psi,\phi)=\sum_{l=0}^{\infty}\sum_{m=-l}^{l}\sum_{n=-l}^{l} W_{lmn}Z_{lmn}(\xi)e^{-im\psi}e^{-in\phi}. \tag{8}$$

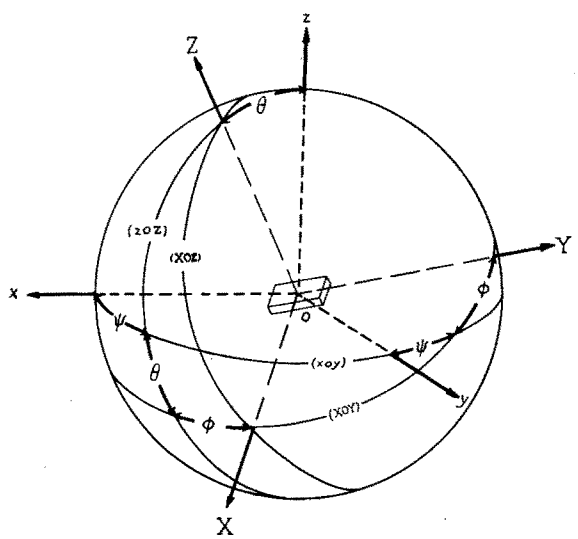

FIG. 1. Diagram illustrating the Eulerian angles ψ, θ, and ϕ which specify the orientation of *crystallite* coordinate system 0-XYZ with respect to *sample* coordinate system 0-xyz.

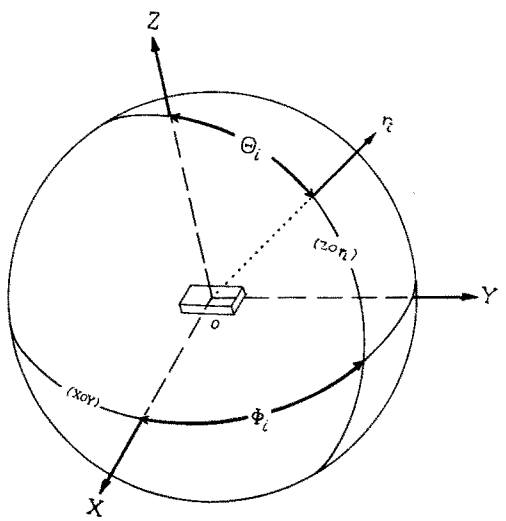

FIG. 2. Diagram illustrating the angles Θ_i and Φ_i which specify the orientation of a reciprocal lattice vector $\mathbf{r}_i$ with respect to *crystallite* coordinate system 0-XYZ.

[9] R. H. Bragg and C. M. Packer, J. Appl. Phys. **35**, 1322 (1964).

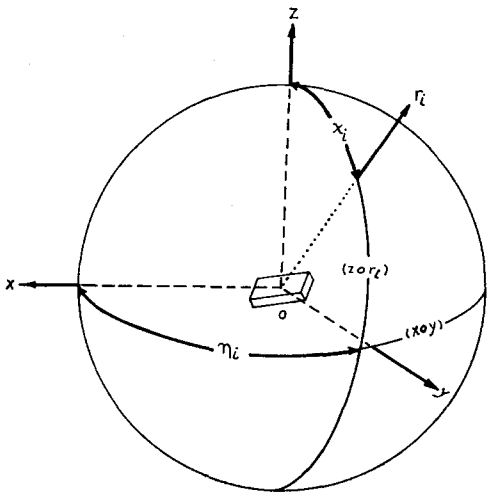

FIG. 3. Diagram illustrating the angles χ_i and η_i which specify the orientation of a reciprocal lattice vector $\mathbf{r}_i$ with respect to *sample* coordinate system 0-*xyz*.

Here $P_l^m(\zeta)$ is the *normalized* associated Legendre function, and $Z_{lmn}(\xi)$, defined in Appendix, is a generalization of the associated Legendre function. The coefficients $Q_{lm}{}^i$ and W_{lmn} can be determined by

$$Q_{lm}{}^i=\frac{1}{2\pi}\int_0^{2\pi}\int_{-1}^{1} q_i(\zeta_i,\eta_i)P_l^m(\zeta_i)e^{im\eta_i}d\zeta_i d\eta_i \quad (9)$$

and

$$W_{lmn}=\frac{1}{4\pi^2}\int_0^{2\pi}\int_0^{2\pi}\int_{-1}^{1} w(\xi,\psi,\phi)Z_{lmn}(\xi) \times e^{im\psi}e^{in\phi}d\xi d\psi d\phi. \quad (10)$$

The establishment of the relation between $w(\xi,\psi,\phi)$ and the set of $q_i(\zeta_i,\eta_i)$ then amounts to finding the relation between the two sets of coefficients W_{lmn} and $Q_{lm}{}^i$.

One can show[10] that Eq. (3) is equivalent to

$$P_l^m(\zeta_i)e^{im\eta_i}=\left(\frac{2}{2l+1}\right)^{\frac{1}{2}}\sum_{n=-l}^{l} Z_{lmn}(\xi)e^{im\psi}e^{in\phi} \times P_l^n(\Xi_i)e^{in\Phi_i} \quad \begin{pmatrix} l=0,\,1,\,2,\,\cdots \\ m=-l,\,\cdots,\,0,\,\cdots,\,l \end{pmatrix}, \quad (11)$$

where

$$\Xi_i=\cos\Theta_i. \quad (12)$$

Equation (11) is a generalization of the Legendre addition theorem. By multiplying both sides of Eq. (11) by $w(\xi,\psi,\phi)$ $q_i(\zeta_i,\eta_i)$ and integrating over the whole ranges of ξ, ψ, ϕ, ζ_i, and η_i, we obtain

$$Q_{lm}{}^i=(2\pi)\left(\frac{2}{2l+1}\right)^{\frac{1}{2}}\sum_{n=-l}^{l} W_{lmn}P_l^n(\Xi_i)e^{in\Phi_i}. \quad (13)$$

When the values of $Q_{lm}{}^i$ are known, then for fixed values of l, m, and i, (13) is a linear equation (on a complex plane) with $(2l+1)$ unknowns, W_{lmn} $(n=-l,\,\cdots,\,l)$. If measurements are made for $(2l+1)$ reciprocal lattice vectors and the corresponding $Q_{lm}{}^i$ determined, the $(2l+1)$ simultaneous linear equations (with fixed l and m) can then be solved to give W_{lmn}. Conversely, once all the W_{lmn} are known, the function $q_i(\zeta_i,\eta_i)$ for any reciprocal lattice vector $\mathbf{r}_i$ can be obtained through use of (13) and (7). If N is the total number of reciprocal lattice vectors for which $q_i(\zeta_i,\eta_i)$ have been measured, then W_{lmn} can be determined in general for l up to at least $(N-1)/2$, and the crystallite orientation distribution is approximated by a corresponding truncated series instead of the infinite series (8). The error introduced by truncation of the series can be estimated by the method given in Sec. IV. When the sample possesses symmetry elements, many of the W_{lmn} are no longer independent and some of them are identically equal to zero. Thus in most cases the largest value of l, for which W_{lmn} can be determined, far exceeds the minimum $(N-1)/2$. The symmetry properties of the coefficients will be examined in Sec. V.

Although, as stated earlier, the crystallite and sample reference systems, 0-*XYZ* and 0-*xyz*, can be chosen arbitrarily, the full benefit of the simplification arising from symmetry will be realized if the axes are chosen to coincide with as many symmetry elements as possible. If, after all the W_{lmn} have been already determined, it is desired to choose a new crystallite reference system 0-$X'Y'Z'$, the new set of expansion coefficients $W_{lmn}{}'$ can be obtained as a linear combination of W_{lmn}. Suppose the new reference system 0-$X'Y'Z'$ is obtained by rotation of 0-*XYZ* by α, β, and γ, the latter being the three Eulerian angles defined in the sense of Margenau and Murphy.[8] If we denote the polar and azimuthal angles of $\mathbf{r}_i$ with respect to 0-$X'Y'Z'$ by Θ_i' and Φ_i', then

$$\begin{bmatrix} \sin\Theta_i\cos\Phi_i \\ \sin\Theta_i\sin\Phi_i \\ \cos\Theta_i \end{bmatrix} = \mathbf{T}^{-1}(\alpha,\beta,\gamma)\begin{bmatrix} \sin\Theta_i'\cos\Phi_i' \\ \sin\Theta_i'\sin\Phi_i' \\ \cos\Theta_i' \end{bmatrix} \quad (14)$$

which leads to

$$P_l^p(\Xi_i)e^{ip\Phi_i}=\left(\frac{2}{2l+1}\right)^{\frac{1}{2}}\sum_{n=-l}^{l} Z_{lpn}(\cos\beta)e^{ip\alpha}e^{in\gamma} \times P_l^n(\Xi_i')e^{in\Phi_i'}. \quad (15)$$

Substitution of (15) into (13) then gives

$$W_{lmn}{}'=\left(\frac{2}{2l+1}\right)^{\frac{1}{2}}\sum_{p=-l}^{l} W_{lmp}Z_{lpn}(\cos\beta)e^{ip\alpha}e^{in\gamma}. \quad (16)$$

Similarly, if the sample reference system 0-*xyz* is rotated by α,β,γ, the expansion coefficients $W_{lmn}{}''$ of the crystallite orientation distribution referred to this new system is given by

$$W_{lmn}{}''=\left(\frac{2}{2l+1}\right)^{\frac{1}{2}}\sum_{p=-l}^{l} W_{lpn}Z_{lpm}(\cos\beta)e^{-ip\alpha}e^{-im\gamma}. \quad (17)$$

[10] M. E. Rose, *Elementary Theory of Angular Momentum* (John Wiley & Sons, Inc., New York, 1957), Chap. 4.

For the purpose of computation it is more convenient to have equations involving real quantities only. If we write

$$W_{lmn}=A_{lmn}+iB_{lmn} \tag{18}$$

$$Q_{lm}{}^{i}=\alpha_{lm}{}^{i}+i\beta_{lm}{}^{i}, \tag{19}$$

then Eqs. (7), (8), and (13) can be re-written in the following forms:

$$q_i(\zeta_i,\eta_i)=\sum_{l=0}^{\infty}\sum_{m=-l}^{l}P_l{}^{m}(\zeta_i)\times[\alpha_{lm}{}^{i}\cos m\eta_i+\beta_{lm}{}^{i}\sin m\eta_i], \tag{7a}$$

$$w(\xi,\psi,\phi)=\sum_{l=0}^{\infty}\sum_{m=-l}^{l}\sum_{n=-l}^{l}Z_{lmn}(\xi)[A_{lmn}\cos(m\psi+n\phi)+B_{lmn}\sin(m\psi+n\phi)], \tag{8a}$$

$$\alpha_{lm}{}^{i}=(2\pi)\left(\frac{2}{2l+1}\right)^{\frac{1}{2}}\sum_{n=-l}^{l}P_l{}^{n}(\Xi_i)\times[A_{lmn}\cos n\Phi_i-B_{lmn}\sin n\Phi_i], \tag{13a}$$[11]

$$\beta_{lm}{}^{i}=(2\pi)\left(\frac{2}{2l+1}\right)^{\frac{1}{2}}\sum_{n=-l}^{l}P_l{}^{n}(\Xi_i)\times[A_{lmn}\sin n\Phi_i+B_{lmn}\cos n\Phi_i]. \tag{13b}$$

The number of terms in the above four equations can in fact be much smaller than those indicated by the forms of the equations, since the symmetry relation existing among the real expansion coefficients was not taken into account explicitly in writing them. Because of the symmetry properties of $P_l{}^{m}(z)$ and $Z_{lmn}(z)$ given in Appendix, we see from (9) and (10) that

$$\left.\begin{aligned}Q_{lm}&=(-1)^{m}Q_{l\bar{m}}{}^{*}\\ \alpha_{lm}&=(-1)^{m}\alpha_{l\bar{m}}\\ \beta_{lm}&=(-1)^{m+1}\beta_{l\bar{m}}\end{aligned}\right\} \tag{20}$$

and

$$\left.\begin{aligned}W_{lmn}&=(-1)^{m+n}W_{l\bar{m}\bar{n}}{}^{*}\\ A_{lmn}&=(-1)^{m+n}A_{l\bar{m}\bar{n}}\\ B_{lmn}&=(-1)^{m+n+1}B_{l\bar{m}\bar{n}}\end{aligned}\right\}, \tag{21}$$

where $\bar{m}=-m$ and * denotes the complex conjugate. More symmetry relations among the coefficients will arise if the sample possesses crystallographic and statistical symmetry elements.

III. METHODS OF IMPROVING THE ACCURACY

Aside from the error arising from truncation of the series in Eq. (8), the accuracy of the function $w(\xi,\psi,\phi)$ is affected by experimental errors in determining the plane-normal distributions $q_i(\zeta_i,\eta_i)$. Three useful procedures for minimizing the latter effect are described here.

The discussion in Sec. II was based on the tacit assumption that the function $q_i(\zeta_i,\eta_i)$ obtained by normalization of intensity distribution [Eq. (16)] represents the true orientation distribution of a given plane-normal. A cause of deviation from this idealization, encountered more frequently in the case of polymers, is the smearing effect due to line broadening. When the crystallites are very small and imperfect, the reflection from a set of the ith crystallographic planes belonging to a *single* crystallite is no longer sharp, but gives rise to a smeared distribution of x-ray intensities, which has a maximum at the particular setting of the diffractometer geometry corresponding to $\Theta_i{}^{\circ}$, $\Phi_i{}^{\circ}$, and $r_i{}^{\circ}$ computed from the idealized unit cell dimensions. In other words the reciprocal lattice belonging to $\mathbf{r}_i$ is no longer a geometric point but occupies a finite volume in the reciprocal lattice space. Suppose then that we know or can estimate the distribution of the density of the reciprocal lattice belonging to $\mathbf{r}_i$, and represent it by $h_i{}^{\circ}(\Xi_i,\Phi_i,r_i)$. Since here we are not concerned with line broadening with respect to the Bragg angle, it is convenient to redefine the reciprocal lattice density distribution function $h_i(\Xi_i,\Phi_i)$ by

$$h_i(\Xi_i,\Phi_i)=\int_{\Delta r_i}h_i{}^{\circ}(\Xi_i,\Phi_i,r_i)dr_i \tag{22a}$$

or

$$h_i(\Xi_i,\Phi_i)\propto h_i{}^{\circ}(\Xi_i,\Phi_i,r_i{}^{\circ}), \tag{22b}$$

depending on whether the intensity data are collected by integrating over a range of Bragg angles or at the peak Bragg angle. If we now multiply both sides of Eq. (13) with $h_i(\Xi_i,\Phi_i)$ and integrate over the whole ranges of Ξ_i and Φ_i, then [assuming the normalization of the $h_i(\Xi_i,\Phi_i)$ function] we obtain

$$Q_{lm}{}^{i}=(2\pi)^{2}\left(\frac{2}{2l+1}\right)^{\frac{1}{2}}\sum_{n=-l}^{l}W_{lmn}H_{ln}{}^{i}, \tag{23}$$

where

$$H_{ln}{}^{i}=\frac{1}{2\pi}\int_{0}^{2\pi}\int_{-1}^{1}P_l{}^{n}(\Xi_i)e^{in\Phi_i}h_i(\Xi_i,\Phi_i)d\Xi_i d\Phi_i. \tag{24}$$

The coefficients W_{lmn} can now be determined by solving the system of linear equations (23) ($i=1,\cdots,N$) instead of (13). Equations corresponding to (13a) and (13b) can be obtained by decomposing $H_{ln}{}^{i}$ into a real and imaginary part.

Next, if the reciprocal lattice vector $\mathbf{r}_i$ is composite[6,12] in the sense that there are several independent reciprocal lattice vectors $\mathbf{r}_{i1}, \mathbf{r}_{i2}, \cdots, \mathbf{r}_{ij}$ having so nearly the same Bragg angle that they cannot be resolved, then we can define the composite distribution of reciprocal lattice density by

$$h_i(\Xi_i,\Phi_i)=\sum_j C_{ij}h_{ij}(\Xi_i,\Phi_i), \tag{25}$$

where

$$C_{ij}=(F_{ij})^{2}/\sum_j(F_{ij})^{2}, \tag{26}$$

[11] Equation (11a) of Part I[6] contains an error. The + sign in front of B_{lm} ought to be replaced by a − sign.

[12] R. A. Sack, J. Polymer Sci. 54, 543 (1961).

F_{ij} being the structure factor of $\mathbf{r}_{ij}$. Then Eq. (23) still holds with the modification that

$$H_{ln}{}^{i}=\sum_{j} C_{ij}H_{ln}{}^{ij} \tag{27}$$

with $H_{ln}{}^{ij}$ defined analogous to Eq. (24).

Finally we can employ the method of least squares[6,12] to solve the over-determined linear equations (23) when N is larger than the number of unknowns W_{lmn}. If we assign a weighting factor ρ_i to each observed $q_i(\zeta_i,\eta_i)$ according to its estimated accuracy, then by applying the standard least-squares criterion we obtain a new set of simultaneous equations

$$\sum_{i=1}^{N}\rho_i Q_{lm}{}^{i}H_{l\nu}{}^{i*}=(2\pi)^2\left(\frac{2}{2l+1}\right)^{\frac{1}{2}}\sum_{n=-l}^{l}W_{lmn}\times\sum_{i=1}^{N}\rho_i H_{ln}{}^{i}H_{l\nu}{}^{i*}\quad(\nu=-l,\cdots,l). \tag{28}$$

If the sample possesses symmetry, Eq. (28) is simplified accordingly and the number of equations in the set is reduced. Decomposing Eq. (28) into a real and imaginary part, one can easily obtain corresponding equations involving real quantities only.

IV. ESTIMATING THE TRUNCATION ERROR

The general line of discussion presented in the previous paper[6] for estimating the series truncation error can be applied to the present, more general case without any major modifications. Only a brief outline is given below, mainly in order to list the revised equations appropriate to the generalization.

If in the series expansion of $q(\zeta,\eta)$ in Eq. (7) all the terms with l higher than λ are arbitrarily neglected, then the standard deviation σ_q of the truncated series can be determined by

$$\sigma_q{}^2=\int_0^{2\pi}\int_{-1}^{1}\left[q(\zeta,\eta)-\sum_{l=0}^{\lambda}\sum_{m=-l}^{l}Q_{lm}P_l{}^{m}(\zeta)e^{-im\eta}\right]^2d\zeta d\eta \tag{29}$$

$$=\int_0^{2\pi}\int_{-1}^{1}\left[q(\zeta,\eta)\right]^2d\zeta d\eta-(2\pi)\sum_{l=0}^{\lambda}\sum_{m=-l}^{l}Q_{lm}Q_{lm}{}^{*}, \tag{30}$$

where the first term in (30) can be evaluated numerically by integrating the square of the observed $q(\zeta,\eta)$ function. Next we want to represent the truncation error in $w(\xi,\psi,\phi)$ by the standard deviation σ_w which is defined by

$$\sigma_w{}^2=\int_0^{2\pi}\int_0^{2\pi}\int_{-1}^{1}\left[w(\xi,\psi,\phi)-\sum_{l=0}^{\lambda}\sum_{m=-l}^{l}\sum_{n=-l}^{l}W_{lmn}Z_{lmn}(\xi)\times e^{-im\psi}e^{-in\phi}\right]^2d\xi d\psi d\phi \tag{31}$$

$$=4\pi^2\sum_{l=\lambda+1}^{\infty}\sum_{m=-l}^{l}\sum_{n=-l}^{l}W_{lmn}W_{lmn}{}^{*}. \tag{32}$$

An approximate estimate of the quantity in (32) can be obtained by the following consideration. We first consider the value of $Q_{lm}Q_{lm}{}^{*}$ averaged over all reciprocal lattice vectors accessible to measurement. If we make the approximation that these vectors are fairly uniformly distributed with respect to Ξ and Φ, then it can be shown[6] by use of Eq. (13) that the following relation holds:

$$\langle Q_{lm}Q_{lm}{}^{*}\rangle\cong 2\pi^2\left(\frac{2}{2l+1}\right)\sum_{n=-l}^{l}W_{lmn}W_{lmn}{}^{*}. \tag{33}$$

Substitution of (33) into (32) leads then to

$$\sigma_w{}^2\cong 2\sum_{l=\lambda+1}^{\infty}\frac{2l+1}{2}\sum_{m=-l}^{l}\langle Q_{lm}Q_{lm}{}^{*}\rangle. \tag{34}$$

The sum at the right-hand side of (34) can in principle be evaluated from experimental data up to any desired value of l, although in practice it might be more convenient to resort to an extrapolation procedure similar to that employed in Part II.[7]

V. CONSEQUENCES OF SYMMETRY

The amount of computation required to obtain $w(\xi,\psi,\phi)$ is frequently much smaller than is apparent from the previous equations, if we take into account symmetry relations existing among the coefficients.

Friedel's law requires that the observed diffraction data always possess centrosymmetry. In other words, the relation

$$q(\zeta,\eta)=q(-\zeta,\eta+\pi) \tag{35}$$

holds identically. Expanding both sides of (35) in a series of spherical harmonics and utilizing the property of associated Legendre functions

$$P_l{}^{m}(-\zeta)=(-1)^{l+m}P_l{}^{m}(\zeta), \tag{36}$$

we find that

$$Q_{lm}=(-1)^{l}Q_{lm} \tag{37}$$

This requires Q_{lm} be identically zero when l is odd. Since in Eq. (13) Q_{lm} is given as a linear combination of W_{lmn} with arbitrary coefficients, we further conclude that W_{lmn} is also identically equal to zero when l is odd. In the discussions to follow it will be understood that only coefficients with even values of l are being considered.

Certain types of symmetry elements in the statistical distribution of crystallites are introduced into the sample in its fabrication process regardless of the nature of crystallites. For example, in a uniaxially stretched sample there is cylindrical symmetry around the axis. Again, when a material is stressed in two mutually perpendicular directions, the sample will have a set of three mutually perpendicular mirror planes. The consequences of these statistical symmetry elements on the symmetry properties of $q(\zeta,\eta)$, Q_{lm}, and W_{lmn} are listed in Table I. Most sheet or film samples encountered in

TABLE I. Symmetry properties of Q_{lm} and W_{lmn} arising from statistical symmetry of crystallite distribution.

Statistical symmetry element	$q(\zeta,\eta)$	Q_{lm}	W_{lmn}
Mirror $\perp x$	$=q(\zeta,\pi-\eta)$	$=Q_{l\bar{m}}$	$=W_{l\bar{m}n}=(-1)^{m+n}W^*_{lm\bar{n}}$
Mirror $\perp y$	$=q(\zeta,-\eta)$	$=(-1)^mQ_{l\bar{m}}$	$=(-1)^mW_{l\bar{m}n}=(-1)^nW^*_{lm\bar{n}}$
Mirror $\perp z$	$=q(-\zeta,\eta)$	$\begin{cases}\neq 0, & m \text{ even}\\ =0, & m \text{ odd}\end{cases}$	$\begin{cases}\neq 0, & m \text{ even}\\ =0, & m \text{ odd}\end{cases}$
All these mirrors present		$\begin{cases}=Q_{lm}, & m \text{ even}\\ =0, & m \text{ odd}\end{cases}$	$\begin{cases}=W_{l\bar{m}n}=(-1)^nW^*_{lm\bar{n}}, & m \text{ even}\\ =0, & m \text{ odd}\end{cases}$
Cylindrical symmetry around z	$=q(\zeta,0)$	$\begin{cases}\neq 0, & m=0\\ =0, & m\neq 0\end{cases}$	$\begin{cases}\neq 0, & m=0\\ =0, & m\neq 0\end{cases}$

practice have the orthogonal biaxial symmetry and in such cases we have all Q_{lm} and W_{lmn} equal to zero when m is odd, and moreover

$$\left.\begin{aligned}&\alpha_{lm}=\alpha_{l\bar{m}}\\&\beta_{lm}=0\\&A_{lmn}=A_{l\bar{m}n}=(-1)^nA_{lm\bar{n}}=(-1)^nA_{l\bar{m}\bar{n}}\\&B_{lmn}=B_{l\bar{m}n}=(-1)^{n+1}B_{lm\bar{n}}=(-1)^{n+1}B_{l\bar{m}\bar{n}}\end{aligned}\right\}(m \text{ even}). \tag{38}$$

The crystallographic symmetry elements existing in the individual crystallites again impose symmetry properties to the W_{lmn} coefficients. If the crystallites possess a mirror plane of symmetry perpendicular to the X axis, then two reciprocal lattice vectors having coordinates (Θ,Φ) and $(\Theta,\pi-\Phi)$ are equivalent, giving rise to identical plane-normal distributions. Substituting these angular coordinates of the two vectors in turn in (13) and comparing the resulting two expressions, we find the following relation to hold:

$$W_{lmn}=(-1)^nW_{lm\bar{n}}. \tag{39}$$

The consequences of various crystallographic symmetry elements, worked out in the similar way, are listed in Table II. By combining the symmetry elements listed in the table, we find, for example, that orthorhombic crystals will demand

$$\left.\begin{aligned}W_{lmn}&=W_{lm\bar{n}} \quad n \text{ even}\\&=0 \quad\quad n \text{ odd}\end{aligned}\right\}. \tag{40}$$

If, in addition, the sample has orthogonal statistical symmetry as in films, then the overlap of the two kinds of symmetry imposes the requirement that W_{lmn} is real and vanishes unless both m and n are even.

VI. DISCUSSION

The procedures required in practice to obtain the crystallite orientation distribution of samples having fiber symmetry were outlined in Part I[6] and were illustrated with their application to polyethylene data in Part II.[7] The basis steps require for application of the present generalized method remain essentially the same. The amount of data and computation will of course have to be considerably greater when the simplifying restriction of fiber symmetry is removed. The increase in labor parallels that of going from two-dimensional to three-dimensional Fourier synthesis in crystal structure analysis. The current improvement in x-ray diffraction apparatus, especially automation of intensity data collection, and easier access to fast, large-scale electronic computers bring the application of the present method well within the realm of practicability. The coefficients of Jacobi polynomials appearing in the $Z_{lmn}(z)$ functions can easily be generated and stored in a computer.

When a complete description of the crystallite orientation distribution is not desired, the present method can still be utilized to obtain W_{lmn} for low values of l only. The frequent practice of characterizing orientation of crystallites by $\langle\cos^2\theta\rangle$ alone amounts to evaluating only W_{200}. W_{lmn}, in effect, represents the value of a certain polynomial of trigonometric functions of θ,ψ, and ϕ, averaged over all orientations of crystallites [see Eq. (10)], and the evaluation of a limited number of W_{lmn} corresponds to the common procedure of specifying a distribution function by the first few of its "moments."

Jetter, McHargue, and Williams[4] indicated that the crystallite orientation distribution in rolled sheets might be specified by a set of two inverse pole figures, each describing the distribution of a specified reference axis of the sample such as rolling and transverse directions. Each of these can in practice be obtained[4] by constructing the inverse pole figure from x-ray data which were rendered to have fiber symmetry by rotating the sheet sample rapidly around the reference axis. The inverse

TABLE II. Symmetry properties of W_{lmn} arising from crystallographic symmetry of crystallites.

Crystallographic symmetry element	Vector equivalent to (Θ,Φ)	W_{lmn}
Mirror $\perp X$	$(\Theta,\pi-\Phi)$	$=(-1)^nW_{l\bar{m}n}=(-1)^mW^*_{l\bar{m}n}$
Mirror $\perp Y$	$(\Theta,-\Phi)$	$=W_{lm\bar{n}}=(-1)^{m+n}W^*_{l\bar{m}n}$
Mirror $\perp Z$	$(\pi-\Theta,\Phi)$	$\begin{cases}\neq 0, & n \text{ even}\\ =0, & n \text{ odd}\end{cases}$
r-fold rotation symmetry around Z	$\left(\Theta,\Phi+2\pi\frac{j}{r}\right)$ $(j=1,2,\cdots,r-1)$	$\begin{cases}\neq 0, & n \text{ is multiple of } r\\ =0, & \text{otherwise}\end{cases}$

pole figure thus obtained by deliberate averaging, then, corresponds to the simplified function obtained by integrating $w(\xi,\psi,\phi)$ with respect to ψ. It is, however, not any more informative than any single pole figure or plane-normal distribution, since the latter can be obtained in effect by line-integration of $w(\xi,\psi,\phi)$ along a certain path. It is then clear[3] that a collection of a finite number of these restricted inverse pole figure cannot provide a full description of poycrystalline texture, in much the same sense that a collection of pole figure diagrams itself does not reveal the same directly. In this connection we might mention that the term "inverse pole figure" is not a logical one for describing any possible graphical representation of the crystallite orientation distribution for samples not having fiber symmetry. For, in such instances, the orientation of the sample reference axes with respect to the crystallographic axes can no longer be represented by a pole on a unit sphere but requires the further specification of a third parameter.

The reciprocal lattice density distribution or the "smearing" function $h(\Xi,\Phi)$ (Sec. III) is usually not known beforehand. However, if we assume a spherically symmetric distribution of the density in the reciprocal space around the "ideal" lattice point, then we may be able to estimate $h(\Xi,\Phi)$ from the observed linebroadening in the Bragg angle direction. Or conversely, one may express $h(\Xi,\Phi)$ by an empirical equation containing a few adjustable parameters and then find the best values of these parameters by trial and error until the two sets of $Q_{lm}{}^{i}$, that is, one obtained directly from experimentally observed $q_i(\zeta_i,\eta_i)$ by use of (9) and the other recovered from $w(\xi,\psi,\phi)$ by use of (13), attain best agreement with each other. This can be done in the same way as the component contributions C_{ij} to a composite plane-normal distribution were adjusted by trial and error in Part II.[7] The smearing function thus obtained may shed some light on the strain-induced modification of the size and lattice structure of the crystallite. The smearing function in the present method plays, in a way, the role of the temperature factor arising in crystal structure determination by Fourier synthesis.

APPENDIX

The function $Z_{lmn}(\xi)$ is given by a solution of the differential equation

$$(1-\xi^2)\frac{d^2Z}{d\xi^2}-2\xi\frac{dZ}{d\xi}+\left[l(l+1)-\frac{m^2-2mn\xi+n^2}{1-\xi^2}\right]Z=0. \quad \text{(A1)}$$

By making the substitutions

$$t=(1-\xi)/2, \quad \text{(A2)}$$

$$Z=Nt^{(m-n)/2}(1-t)^{(m+n)/2}f(t) \quad \text{(A3)}$$

into (A1), we obtain

$$t(t-1)(d^2f/dt^2)+[(m-n+1)-2mt](df/dt)+[l(l+1)-m(m+1)]f=0. \quad \text{(A4)}$$

A solution to (A4), when $m\geqslant n$, is given by

$$f(t)={}_2F_1(-l+m,\, l+m+1;\, m-n+1;\, t) \quad (m\geqslant n), \quad \text{(A5)}$$

where ${}_2F_1$ is the hypergeometric function defined by

$${}_2F_1(\alpha,\beta;\gamma;t)=1+\frac{\alpha\cdot\beta}{1\cdot\gamma}t+\frac{\alpha(\alpha+1)\beta(\beta+1)}{2!\gamma(\gamma+1)}t^2+\cdots. \quad \text{(A6)}$$

When α is a negative integer, the series in (A6) terminates after a finite number of terms and the resulting polynomial is called a Jacobi polynomial.[13,14a] The constant N in (A3) is determined from the normalization condition

$$\int_{-1}^{1} Z_{lmn}{}^2(\xi)d\xi=1 \quad \text{(A7)}$$

so that[10]

$$N_{lmn}{}^2=\left(\frac{2l+1}{2}\right)\frac{(l+m)!(l-n)!}{(l-m)!(l+n)!}\frac{1}{[(m-n)!]^2}. \quad \text{(A8)}$$

When $m\geqslant n$, the relation $-n\geqslant -m$ holds. Then replacing m and n in (A3), (A5), and (A8) by $-n$ and $-m$, respectively, and utilizing the relation[15]

$${}_2F_1(\alpha,\beta;\gamma;t)=(1-t)^{\gamma-\alpha-\beta}{}_2F_1(\gamma-\beta,\,\gamma-\alpha;\,\gamma;\,t), \quad \text{(A9)}$$

we find that

$$Z_{lmn}=Z_{l\bar{n}\bar{m}}. \quad \text{(A10)}$$

In order to find Z_{lmn} for $m<n$ we note that equation (A1) is unchanged when m and n are interchanged. Thus the solution Z_{lmn} is identical to $\pm Z_{lnm}$. The ambiguity with respect to the sign arises because the normalization procedure (A7) does not determine the sign uniquely. We then adopt the convention that

$$Z_{lmn}=(-1)^{m+n}Z_{lnm} \quad \text{(A11)}$$

from which it follows that

$$Z_{lmn}=(-1)^{m+n}Z_{l\bar{m}\bar{n}}. \quad \text{(A12)}$$

The Jacobi polynomial (A5) is also obtained by orthogonalization of polynomials with respect to the weight function[13]:

$$p(t)=t^{(m-n)/2}(1-t)^{(m+n)/2} \quad \text{(A13)}$$

in the interval $0\leqslant t\leqslant 1$. It thus follows that Z_{lmn} functions satisfy the orthogonal relation

$$\int_{-1}^{1} Z_{lmn}(\xi)Z_{l'mn}(\xi)d\xi=\delta_{ll'}. \quad \text{(A14)}$$

[13] R. Courant and D. Hilbert, *Methods of Mathematical Physics* (Interscience Publishers, Inc., New York, 1953).
[14] H. Margenau and G. M. Murphy, Ref. 8 (a) p. 213, (b) Chap. 15.
[15] I. N. Sneddon, *Special Functions of Mathematical Physics and Chemistry* (Oliver and Boyd, Edinburgh, 1956).

By putting $n=0$ in (A3), (A5), and (A8) we find that for $m \geqslant 0$

$$P_l^m(\xi)=Z_{lm0}(\xi), \tag{A15}$$

where $P_l^m(\xi)$ is the normalized associated Legendre function. If we consider (A15) as the definition of $P_l^m(\xi)$ even for negative values of m, then because of (A12) we have

$$P_l^m(\xi)=(-1)^m P_l^{\bar{m}}(\xi). \tag{A16}$$

Note that (A16) indicates a deviation from the frequent convention adopted in other works in which $P_l^m(\xi)$ for negative m is defined to be equal to $P_l^{|m|}(\xi)$.

The function Z_{lmn} arises in the Schrödinger wave function of a symmetric rotator[16–18] and in the matrix representation of the rotation groups.[10,14b] Further details on the properties of the function are found in the literature pertaining to these subjects.

ACKNOWLEDGMENTS

Grateful acknowledgment is made to Professor W. R. Krigbaum and Professor W. H. Stockmayer for helpful discussions.

[16] F. Reiche and H. Rademacher, Z. Physik **39**, 444 (1926).
[17] D. M. Dennison, Rev. Mod. Phys. **3**, 280 (1931).
[18] H. H. Nielsen, Rev. Mod. Phys. **23**, 90 (1951).

JOURNAL OF APPLIED PHYSICS VOLUME 36, NUMBER 6 JUNE 1965

Dielectric Properties of Cobalt Oxide, Nickel Oxide, and Their Mixed Crystals*

K. V. Rao and A. Smakula

Electrical Engineering Department—Center for Materials Science and Engineering, Crystal Physics Laboratory, Massachusetts Institute of Technology, Cambridge, Massachusetts

(Received 2 November 1964)

Dielectric constant κ', loss κ'', and conductivity σ of single crystals of CoO, NiO, and mixed crystals of CoO–NiO as a function of frequency from 10^2 to 10^{10} cps and temperature from -193°C to 400°C have been determined. The dielectric constant κ' is constant (12.9 at 25°C) in the whole frequency range in CoO. It decreases with frequency in NiO and mixed crystals CoO–NiO. In NiO κ' reaches a constant value (11.9 at 25°C) at 10^5 cps, and in CoO·NiO (12.3 at 25°C) at 10^{10} cps. The dielectric constants extrapolated to 0°K are 10.9, 10.0, and 9.1 for CoO, CoO·NiO, and NiO, respectively. In all crystals the dielectric constant increases exponentially with temperature. Using modified Debye equations, two thermal activation energies for κ' have been obtained: 0.042, 0.027, and 0.018 eV for temperatures below 40°C (frequency-independent region); 0.33, 0.20, and 0.16 eV for temperatures above 40°C, for CoO, NiO, and CoO·NiO (frequency-dependent region). The plot of log σ vs $1/T$ gives straight lines for CoO from 400° to 100°C, and NiO from 400° to 25°C with activation energies 0.73 and 0.66 eV. At lower temperatures the activation energies decrease continuously. The mixed crystals have two activation energies, one at high temperatures and the other at low temperatures. Variation of the activation energy with composition at high temperatures is less than that at low temperatures. The variation of activation energies in mixed crystals is correlated to lattice distortion and an increase of trivalent ion concentration.

INTRODUCTION

ELECTRICAL conduction in transition metal oxides (particularly Li-doped NiO) and their mixed systems has been studied extensively.[1–4] With its incompletely filled $3d$ shell, pure NiO should be a good conductor, according to the simple energy-band theory, but experimentally it was found to be an insulator with a room-temperature conductivity σ of the order of 10^{-14} $(\Omega\text{-cm})^{-1}$. Verwey and DeBoer[5] and Mott[6] pointed out that the collective-electron treatment used by Bloch[7] and Wilson[8] is not a good approximation here. Using the Heitler–London approximation, starting from the atomic wave functions, the poor conductivity of NiO can be explained.

When NiO deviates from stoichiometry, either due to a deficiency of Ni or an addition of Li, it becomes a semiconductor with σ varying from 10^{-7} to 10^{-1} $(\Omega\text{-cm})^{-1}$. The activation energy H obtained from the slope of the log σ vs $1/T$ plot decreases from 0.6 to 0.1 eV with increase in Li concentration in the range from 0.1% to 10%. In both cases (either in nonstoichiometric or Li-doped NiO) Ni^{3+} ions are formed to preserve electrical neutrality. The simultaneous presence of Ni^{3+} and Ni^{2+} allows transfer of an electron from one ion to another. This process requires a certain

* The research reported in this paper was sponsored by the Air Force Cambridge Research Laboratories, U. S. Office of Aerospace Research, under Contract No. AF. 19(628)-395.

[1] F. J. Morin, Phys. Rev. **93**, 1190 and 1199 (1954); Bell System Tech. J. **37**, 1047 (1958).
[2] R. R. Heikes and W. D. Johnston, J. Chem. Phys. **26**, 582 (1957).
[3] S. Van Houten, J. Phys. Chem. Solids **17**, 7 (1960).
[4] J. Yamashita and T. Kurosawa, J. Phys. Chem. Solids **5**, 34 (1958).
[5] J. H. De Boer and E. J. W. Verwey, Proc. Phys. Soc. (London) **49**, extra part 59 (1937).
[6] N. F. Mott, Proc. Phys. Soc. (London) **A62**, 416 (1949).
[7] F. Bloch, Elektronentheorie Metalle, Handbuch Metallphysik Radiol. **6.1**, 226 (1933).
[8] A. H. Wilson, Proc. Roy. Soc. (London) **A133**, 458 (1931).